Title: Nigral and striatal connectivity alterations in asymptomatic *LRRK2* mutation carriers: a magnetic resonance imaging study.

Authors: Dolores Vilas, MD[1]*, Bàrbara Segura, PhD[2]*, Hugo C. Baggio MD, PhD[2], Claustre Pont-Sunyer, MD[1], Yaroslau Compta, MD, PhD[1,3,4], Francesc Valldeoriola, MD, PhD[1,3,4], María José Martí, MD, PhD[1,3,4], María Quintana, PhD[1], Angels Bayés, MD[5], Jorge Hernández-Vara, MD[6], Matilde Calopa, MD[7], Miquel Aguilar, MD[8], Carme Junqué, MD, PhD[2,3,4], Eduardo Tolosa, MD, PhD[1,3,4] and the Barcelona LRRK2 Study Group[9].

* These authors contributed equally to the manuscript.

Author's affiliations:

[1]Movement Disorders Unit, Neurology Service, Hospital Clínic de Barcelona, Barcelona, Catalonia, Spain. [2]Psychiatry and Clinical Psychobiology Department, Universitat de Barcelona. Barcelona, Catalonia, Spain. [3]Institut d'Investigacions Biomèdiques August Pi i Sunyer (IDIBAPS), Barcelona, Catalonia, Spain. [4]Centro de Investigación Biomédica en Red sobre Enfermedades Neurodegenerativas (CIBERNED), Hospital Clínic de Barcelona, Barcelona, Catalonia, Spain. [5] Parkinson's Unit, Clínica Teknon, Barcelona, Spain. [6] Neurology Service, Hospital Universitari Vall D'Hebron, Barcelona, Catalonia, Spain. [7]Neurology Service, Hospital Universitari de Bellvitge, Barcelona, Catalonia, Spain. [8]Neurology Service, Hospital Universitari Mutua de Terrasa, Barcelona, Catalonia, Spain. [9]Collaborators listed at end of manuscript.

Corresponding author: Eduardo Tolosa, Neurology Service, Hospital Clínic Barcelona, C/Villarroel 170, 08036 Barcelona, Phone: +34 93 2275785, Fax: +34 93 2275783, email: etolosa@clinic.ub.es

Conflict of interest: None of the authors of this manuscript report conflict of interest.

Word count: 2945

Running title: Functional connectivity in asymptomatic *LRRK2* mutation carriers.

Key words: LRRK2, Parkinson's disease, functional MRI, connectivity.

Funding sources: none.

Email addresses of all authors:

dvilas@clinic.ub.es, segura.barbara@gmail.com, hbaggio@ub.edu,

mcpont@clinic.ub.es, YCOMPTA@clinic.ub.es, FVALLDE@clinic.ub.es,

MJMARTI@clinic.ub.es

mquintanaaparicio@gmail.com, 11741abr@comb.cat

hernandezvarajorge76@gmail.com, mcalopa@bellvitgehospital.cat,

miquelaguilar@gmail.com, cjunque@ub.edu, ETOLOSA@clinic.ub.es

Abstract

Background. The study of the functional connectivity by means of magnetic resonance imaging (MRI) in asymptomatic *LRRK2* mutation carriers could contribute to the characterization of the prediagnostic phase of *LRRK2* associated Parkinson's disease (PD).

Objective. To characterize MRI functional patterns during resting state in asymptomatic *LRRK2* mutation carriers.

Methods. We acquired structural and functional MRI data of 18 asymptomatic *LRRK2* mutation carriers and 18 asymptomatic *LRRK2* mutation noncarriers, all first-degree relatives of *LRRK2*-PD patients. Starting from resting state data, we analyzed the functional connectivity of the striatocortical and the nigrocortical circuitry. Structural brain data was analyzed by voxel based morphometry, cortical thickness and volumetric measures.

Results: Asymptomatic *LRRK2* mutation carriers had functional connectivity reductions between the caudal motor part of the left striatum and ipsilateral precuneus and superior parietal lobe. Connectivity in these regions correlated with subcortical gray matter volumes in mutation carriers. Asymptomatic carriers also showed increased connectivity between the right substantia nigra and bilateral occipital cortical regions (occipital pole and cuneus bilaterally, and right lateral occipital cortex). No intergroup differences in structural MRI measures were found. In *LRRK2* mutation carriers, age and functional connectivity correlated negatively with striatal volumes. Additional analyses including only subjects with the G2019S mutation revealed similar findings.

Conclusion: Asymptomatic *LRRK2* mutation carriers showed functional connectivity changes in striatocortical and nigrocortical circuits compared with noncarriers. These

findings support the concept that altered brain connectivity precedes the onset of classical motor features in a genetic form of PD.

Background

Mutations in the leucine-rich repeat kinase 2 gene (*LRRK2*) are the most common known cause of inherited Parkinson's disease (PD). Potential disease modification treatments for *LRRK2*-PD, such as *LRRK2* kinase inhibitors, are currently under intense study[1]. If effective, it is hoped that these treatments could also have a positive effect in sporadic PD cases since *LRRK2*-PD is clinically similar to sporadic PD and responds to the same therapies.

It is now widely accepted that a prolonged prodromal phase antedates the onset of motor manifestations in sporadic as well as in genetic forms of PD[2]. Still while clinical abnormalities have been reported in prediagnostic *LRRK2*-PD[3-8], most studies suggest that the *LRRK2* prodromic phase could be clinically quite silent. Imaging studies are therefore particularly important in the identification of subjects in this phase of *LRRK2*-PD.

Magnetic resonance imaging (MRI) techniques have demonstrated structural and functional abnormalities in asymptomatic *LRRK2* mutation carriers[8-12]. In structural MRI analyses, gray matter (GM) volume increases have been reported in the caudate nucleus[9] and in the cuneus[10], and decreases in the right prefrontal and orbitofrontal regions[9]. Task based functional MRI (fMRI) results in these subjects have shown changes in imagery-related activity in different cortical and subcortical brain areas[11-12]. Only one study assessed resting state functional connectivity in asymptomatic *LRRK2* mutation carriers by means of functional MRI (fMRI)[13]. In this study, asymptomatic *LRRK2* mutation carriers showed reduced interaction between the right inferior parietal cortex and the dorsoposterior putamen but also an increased interaction of this cortical area with the ventroanterior putamen, suggesting a reorganization of corticostriatal circuits in these subjects.

The aim of the current work was to evaluate whole-brain resting-state functional connectivity and structural brain measures in a group of asymptomatic *LRRK2* mutation carriers. We hypothesized that functional nigral and striatal connectivity might be altered in this group of subjects at high risk of developing PD, a reflection of underlying subclinical brain dysfunction. We also hypothesized that *LRRK2* mutation carriers might show subtle signs of GM structural alteration.

Methods

Participants

Study participants were recruited consecutively between April 2012 and May 2013 among first-degree relatives of a previously-identified cohort of *LRRK2*-PD patients at the Movement Disorders Unit, Hospital Clínic de Barcelona. Exclusion criteria were presence of parkinsonism, other neurodegenerative disorders, and general exclusion criteria for MRI scanning (such as claustrophobia or pacemakers). Thirty-six first-degree relatives of *LRRK2*-PD patients, who came from 17 families, agreed to participate in the study. The presence of a *LRRK2* gene mutation, assessed as previously described[14], was identified in 18 subjects. Among them, 13 (72.2%) were carriers of the G2019S, three (16.7%) of the R1441G, and two (11.1%) of the R1441C mutations. Participants were not aware of their genetic status at the time of the study.

Standard protocol approvals and patient consent

The study was approved by the Ethics Committee of Hospital Clínic de Barcelona (May 2012; code 7723). Written informed consent was obtained from all subjects prior to the study.

Clinical assessment

All study participants were clinically evaluated at a single center by the same researcher team (DV, ET, and CP). Motor signs were assessed through the Movement Disorders Society Unified Parkinson's Disease Rating Scale (MDS-UPDRS-III)[15]. None of the participants showed signs of parkinsonism as determined by neurological examination at the time of the study. Smell was evaluated by means of the 40-item University of Pennsylvania Smell Identification Test (UPSIT; Smell Identification Test™, Sensonics, Spanish version)[16]. The Hospital Anxiety and Depression scale (HADS)[17] and the Beck Depression Inventory-II[18] were used to quantify depression and anxiety symptoms. Dysautonomic features were assessed by means of the SCOPA-AUT scale[19]. Global cognitive function was tested by the Mini-Mental State Examination (MMSE)[20].

Statistical analyses of demographic and clinical data

Normality of distribution of quantitative variables was assessed with the Kolmogorov-Smirnov test. Normally distributed variables were analyzed using independent-samples Student's t tests and Pearson's product-moment correlations; otherwise, Mann-Whitney's U tests and Spearman's rank correlations were used. Qualitative variables were analyzed using Pearson's chi-squared test. Non-imaging statistical

analyses were performed with SPSS version 18.0 (SPSS Inc.) with a two-sided type I error threshold of 5%.

MRI acquisition, processing and analyses

Images for all subjects were obtained with a 3T MRI scanner (MAGNETOM Trio, Siemens, Germany), using an 8-channel head coil. The scanning protocol included a resting-state, 10-min-long functional gradient-echo echo-planar imaging sequence (300 T2*-weighted volumes, TR=2 s, TE=19 ms, flip angle=90º, slice thickness=3 mm, FOV=240 mm, 128x128 matrix), in which subjects were instructed to keep their eyes closed, not to think of anything in particular and not to fall asleep; a high-resolution 3D structural T1-weighted MPRAGE sequence acquired sagittally (TR=2.3 s, TE=2.98 ms, 240 slices, FOV=256 mm; 1 mm isotropic voxel), and a T2-weighted axial FLAIR sequence (TR=9 s and TE=96 ms).

Cortical thickness

The processing pipeline for cortical thickness analyses with FreeSurfer (version 5.3; available at: http://surfer.nmr.harvard.edu) is provided as supplemental data. Comparisons between groups were performed using a vertex-by-vertex general linear model using Qdec. An initial vertex-wise threshold was set at $p<0.05$ to find clusters. To avoid false positives, Monte Carlo simulation with 10,000 repeats was performed. Results are reported at cluster-wise probability significance level set at $p<0.05$.

Subcortical volumetry

Subcortical volumes, including putamen, caudate, and estimated total intracranial volume (eTIV), were obtained automatically via whole-brain segmentation with FreeSurfer.[21]

Voxel-based morphometry

Structural data was analyzed with FSL-VBM[22], a voxel-based morphometry (VBM) style analysis carried out with FSL (release 5.0.4, http://fsl.fmrib.ox.ac.uk/fsl/fslwiki/FSL) (see Supplementary Materials). Voxelwise general linear model was applied, and statistical significance was established through permutation testing (5,000 permutations), randomizing the study groups and generating a sampling distribution of GM volume differences, against which the actual group differences were compared. Statistical significance was set at $p<0.05$, corrected for multiple comparisons using family-wise error (FWE) control.

Processing of fMRI

The preprocessing of resting-state images was performed with FSL and AFNI (http://afni.nimh.nih.gov/afni) tools. Briefly, it included removal of the first 5 volumes to allow for T1 equilibration, grandmean scaling, linear trend removal and temporal filtering (0.01- 0.1 Hz). To control for the effect of head movement and other nonneural sources of signal variation, motion correction and regression of nuisance signals (six motion parameters, cerebrospinal fluid, and white matter) were performed. To remove the effects of timepoints corrupted by motion, a scrubbing procedure[23] was applied, using a root-mean-square interframe intensity difference threshold equal to the 75th percentile + 1.5 times the interquartile range. Additionally, head motion was

calculated as the average Euclidean displacement between consecutive timepoints for rotatory and translatory motion[24].

Definition of regions of interest and extraction of temporal courses

Structures used as regions of interest (ROIs) for seed-based functional connectivity analyses included the substantia nigra and striatum. The striatum was divided into (left and right) caudal motor, rostral motor, executive and limbic regions using the Oxford-GSK-Imanova Striatal Connectivity Atlas (http://fsl.fmrib.ox.ac.uk/fsl/fslwiki/Atlases/striatumconn). Supplementary data includes an analysis of thalamic functional connectivity.

To define the substantia nigra, motion-corrected individual resting-state data sets were temporally averaged and normalized to an MNI template at 2-mm resolution. These normalized images were averaged across subjects, and left and right nigral masks were manually drawn by a trained radiologist (HB) based on the mean image. Supplementary Figure 1 displays the ROI segmentation scheme used.

To obtain each seed region's resting-state time series, their respective masks were linearly registered to each subject's T1-weighted image, and subsequently linearly registered to native functional space using FSL FLIRT. In order to obtain region-specific temporal courses, we initially thresholded each probabilistic mask at 30%, and subsequently extracted a weighted mean of the time series of all voxels inside them in native space, without smoothing.

Functional connectivity analysis

Each seed region's time course was correlated with the time series of every brain voxel using smoothed (6-mm FWHM Gaussian kernel) functional images normalized to MNI space after resampling to 4x4x4 mm^3 voxel size, producing a Pearson's r coefficient correlation map. These were then converted to Z maps using Fisher's r-to-Z transformation. Voxelwise general linear model was applied using non-parametric testing including all brain voxels. Statistical significance was established through permutation testing (5,000 permutations). Significance level was set at $p<0.05$ using threshold-free cluster enhancement[25], corrected for multiple comparisons by controlling the family-wise error (FWE) across space.

In order to assess the relationship between functional connectivity alterations and both clinical and volumetric data, mean connectivity values were obtained by averaging individual Z values in all voxels inside the clusters of significant intergroup differences if results contained more than 10 voxels. Pearson correlation was then used to correlate these values with age, UPDRS-III and UPSIT scores. Additionally, partial correlations were used to correlate age and connectivity values with striatal volumes obtained with FreeSurfer, taking eTIV into account.

Image analysis was performed by independent investigators (BS and HB) blinded to the clinical and genetic status of study subjects.

Results

Demographic and clinical data

Mean age was similar between mutation carriers and noncarriers, with similar ranges (27 to 66 years and 23 to 67 years, respectively) (Table 1). All participants were right-handed. No significant group differences were found in years of education, or UPDRS (I, II or III) and UPSIT scores. Likewise, no significant differences in scores were found for other non-motor features.

Functional connectivity

Asymptomatic *LRRK2* mutation carriers showed differences in functional connectivity compared with asymptomatic noncarriers. Specifically, we found *LRRK2* mutation carriers to have reduced connectivity between the caudal motor subdivision of the left striatum (including the caudal portions of the putamen and caudate nucleus) and the ipsilateral precuneus and superior parietal lobule ($p<0.05$, FWE-corrected) (see Table 2 and Figure 1). *LRRK2* mutation carriers also displayed reduced functional connectivity between the executive subdivision of the left striatum and the anterior-medial part of the superior frontal gyrus (MNI coordinates 6, 54, 24; cluster size 448 mm3; $p=0.036$, FWE-corrected).

Compared with noncarriers, *LRRK2* mutation carriers showed increased functional connectivity between the right substantia nigra and the occipital pole and cuneus bilaterally, and the right lateral occipital cortex (Table 2 and Figure 1).

LRRK2 mutation carriers also displayed reduced functional connectivity between the occipital region of the left thalamus and the occipital cortex bilaterally, including the

occipital pole, calcarine cortex, lateral occipital cortex and lingual gyrus, and the left superior parietal lobule (see supplementary material). Functional connectivity in mutation carriers was also reduced between the temporal part of the left thalamus and bilateral dorsomedial portions of the precentral gyrus, postcentral gyrus and supplementary motor area (see Supplementary Figure 3).

No other significant functional connectivity changes were found when other seed regions were tested. No significant differences in head motion were observed between *LRRK2* mutation carriers and noncarriers (rotation (degrees): carriers 0.03 ± 0.01, noncarriers 0.03 ± 0.02, p=0.662; translation (mm): carriers 0.07 ± 0.03, noncarriers: 0.06 ± 0.05; p=0.445).

Comparisons between G2019S mutation carriers and LRRK2 mutation noncarriers

Structural and functional intergroup analyses excluding the five subjects with *LRRK2* mutations other than G2019S were performed. Thirteen G2019S carriers were contrasted with 18 noncarriers. Functional analyses showed that G2019S mutation carriers had reduced connectivity between the caudal motor subdivision of the left striatum and both the left precuneus and the superior parietal lobule (Figure 2).

G2019S mutation carriers also displayed increased connectivity of the right substantia nigra with the occipital pole and calcarine cortex bilaterally, and with the right lateral occipital cortex (Figure 2).

Differences in thalamic functional connectivity between G2019S mutation carriers and *LRRK2* mutation noncarriers were similar to those observed between overall *LRRK2* mutation carriers and noncarriers (see Supplementary Figure 3).

Correlation between functional connectivity, clinical and structural data

In the carrier group, age significantly correlated with mean connectivity Z scores in the clusters of significant intergroup differences in left caudal motor striatal connectivity (r=-0.475, p=0.046). This effect was not observed in the noncarrier group (r=-0.356, p=0.147).

Techniques such as the Bonferroni method for FWE control involving highly correlated measures (*e.g.*, basal ganglia volumes) can be excessively conservative[26]. We accordingly assessed a possible correlation between connectivity and a single measure, the mean striatal volume, obtained by averaging putaminal and caudate volumes. We observed a significant correlation between Z scores in the clusters of intergroup left caudal motor striatal connectivity differences and this compound striatal volume measure in the carrier group, but not in the noncarrier group (see Table 3 and Figure 1).

Post-hoc correlation analyses between connectivity and volumes of individual striatal nuclei also revealed significant effects in *LRRK2* mutation carriers. In the carrier group, Z scores in the clusters of intergroup left caudal motor striatal connectivity differences correlated positively with bilateral caudate and putamen volumes. No

significant correlations were observed in the noncarrier group (see Figure 1 and Table 3).

No significant correlations were observed between Z scores in the clusters of right substantia nigra connectivity and subcortical volumes. Also, no significant correlations were observed between mean connectivity (in the regions where significant intergroup differences were found) and UPDRS-III or UPSIT scores, either in the whole sample or in the noncarrier or carrier subgroups (all $p>0.2$, uncorrected).

Structural MRI findings

GM volumes (VBM analysis and volumetric measures), cortical thickness measures and eTIV did not differ significantly between groups (Supplementary Table 2). Age correlated significantly and negatively with striatal volumes in the carrier group (especially the putamina), but not in noncarriers (see Table 3).

Discussion

In the present study, asymptomatic *LRRK2* mutation carriers showed resting-state functional connectivity reductions between the left striatum and both the ipsilateral precuneus and superior parietal lobule, and connectivity increments between the right substantia nigra and bilateral occipital cortical regions including the occipital poles and cunei, and the ipsilateral lateral occipital cortex. These connectivity reductions correlated with striatal volumes. Analyses including only subjects with the G2019S mutation revealed similar findings.

In manifest idiopathic PD, reduced corticostriatal functional connectivity has been described in previous resting-state fMRI studies in which decreased connectivity between the thalamus and sensorimotor cortices, [27] and between the striatum and thalamus, midbrain, pons and cerebellum[28] was observed. Even in untreated patients in early stages of idiopathic PD, decreased functional connectivity of the caudate with frontal and insular cortices[29] and in mesolimbic-striatal and corticostriatal loops[30] has been observed.

Information concerning functional connectivity alterations in asymptomatic *LRRK2* carriers is very limited. In healthy G2019S *LRRK2* mutation carriers[13] a resting-state study reported the presence of striatocortical connectivity reorganization. As in the current study, connectivity changes between the posterior striatum and the parietal cortex consisted of positive correlations in mutation noncarriers and negative ones in carriers. In the present study, the striatal connections showing differences between groups were mostly reductions in the functional connectivity in mutation carriers. However, for the nigral connectivity differences, an increase in functional connectivity was observed, occurring between the right substantia nigra and the occipital cortex. Interestingly, increased resting-state functional connectivity between the right substantia nigra and the occipital cortex has been described in patients with idiopathic REM sleep behavior (IRBD) disorder[31], a condition considered to represent prodromal PD[32]. As most IRBD patients are eventually diagnosed with a synucleinopathy, especially PD[32], our findings may represent connectivity changes in prediagnostic PD. In the present study, the striatal connections showing differences between groups are mostly negative for the mutation carriers and positive for the

noncarriers. For the nigral connectivity differences, the opposite pattern was observed. Although the biological significance of negative correlations is controversial[33], different studies revealed that the brain activity is organized into anticorrelated functional networks[34]. The nigral and striatal connectivity alterations observed in our study might reflect a reorganization of these network dynamics, as previously described in patients with idiopathic PD. [35]

In line with our findings in prediagnostic PD, changes in functional connectivity in the have been found in the prediagnostic phase of other neurodegenerative disorders. In Alzheimer's, decreased functional connectivity occurs mainly between the precuneus and limbic regions[36]. In preclinical Huntington's disease, weakened and strengthened connectivity has been observed in the frontostriatal network, thalamus, anterior insula, and memory centers[37]. Although the meaning of these functional changes is unclear, our results suggest that the neurodegenerative process has already started in some of these mutation carriers, leading to brain connectivity changes.

No significant GM atrophy was detected in our asymptomatic mutation carriers, either with VBM or a more sensitive technique such as cortical thickness analysis[38,39]. Correlation analyses, nonetheless, showed that mutation carriers with more marked striatal connectivity reductions tended to have lower striatal volumes, suggesting that *LRRK2* mutation carriers with the lowest levels of striatal connectivity already display subtle signs of neurodegeneration. As *LRRK2* mutation penetrance is age-dependent[3], this hypothesis is in line with the correlation observed between age and both striatal connectivity and striatal volumes in the carrier group. It cannot be ruled out, however, that the observed connectivity reductions (and associated variation in subcortical

volumes) can be at least partially explained by the effect of *LRRK2* mutations. Previous studies showed that the *LRRK2* gene is involved in neuronal morphogenesis as well as striatal synaptic transmission and synaptogenesis during development[40]. The follow-up of these subjects is critical to determine if the observed connectivity reductions or smaller subcortical volumes can predict the occurrence of *LRRK2*-PD. It is difficult to provide an explanation for the laterality of the functional connectivity changes observed in our study. Prospective studies in asymptomatic *LRRK2* mutation carriers may also inform whether the connectivity findings observed reflect the typical asymmetrical pattern of PD initiation and progression.

The small sample size, the lack of behavioral and cognitive assessments, as well as the inclusion of subjects with different *LRRK2* mutations, potentially with different underlying neuropathological substrates, represent limitations when interpreting our results. Similarly, our study did not include either healthy controls unrelated to *LRRK2*-PD patients or a group of symptomatic *LRRK2*-PD patients for comparison purposes. The inclusion of functional and structural analyses can be considered strengths to this study. Structural connectivity techniques could help clarify in future studies the mechanisms underlying the findings observed.

Barcelona *LRRK2* study group

Parkinson's Disease and Movement Disorders Unit, Neurology Service, Institut de Neurociències Hospital Clínic, University of Barcelona: Eduard Tolosa, María José Martí, Yaroslau Compta, Francesc Valldeoriola, Dolores Vilas, Claustre Pont-Sunyer. Neurology Service, Hospital Universitari Germans Trias i Pujol, Badalona: Lourdes Ispierto, Ramiro Álvarez. Neurology Service, Hospital Universitari Vall D'Hebron, Barcelona: Oriol De Fabregues, Jorge Hernández-Vara. Neurology Service, Hospital Del Mar, Barcelona: Víctor Puente. Neurology Service, Hospital Universitari de Bellvitge, Barcelona: Matilde Calopa, Serge Jaumà, Jaume Campdelacreu. Neurology Service, Hospital Universitari Mutua de Terrasa, Barcelona: Miquel Aguilar, Pilar Quílez. Hospital Mateu Orfila, Maó, Menorca: Pilar Casquero.

Acknowledgments

The authors are grateful to the patients and the families for their participation in the study. None of the authors of this manuscript report conflict of interest.

Authors' roles: Dr. Tolosa, Dr. Junqué, Dr. Vilas and Dr. Segura had full access to all the data in the study and take responsibility for the integrity of the data and the accuracy of the data analysis. Dr. Vilas and Dr. Segura: drafting/revising the manuscript, study concept or design, analysis or interpretation of data, acquisition of data, statistical analysis. Dr. Pont-Sunyer, Dr. Compta, Dr. Valldeoriola, Dr. Martí, Dr. Baggio, Dr. Quintana, Dr. Bayés, Dr. Hernández-Vara, Dr. Matilde Calopa, Dr. Aguilar, Dr. Tolosa and Dr. Junqué: drafting/revising the manuscript, study concept or design, analysis or interpretation of data, acquisition of data, study supervision.

References

1. West AB. Ten years and counting: moving leucine-rich repeat kinase 2 inhibitors to the clinic. Mov Disord 2015;30(2):180-9.

2. Tolosa E, Gaig C, Santamaria J, Compta Y. Diagnosis and the premotor phase of Parkinson disease. Neurology 2009;72(7 Suppl):S12-20.

3. Healy DG, Falchi M, O'Sullivan SS, et al. Phenotype, genotype, and worldwide genetic penetrance of LRRK2-associated Parkinson's disease: a case-control study. Lancet Neurol 2008;7(7):583-90.

4. Gaig C, Vilas D, Infante J, et al. Nonmotor symptoms in LRRK2 G2019S associated Parkinson's disease. PLoS One 2014;9(10):e108982.

5. Marras C, Schule B, Munhoz RP, et al. Phenotype in parkinsonian and nonparkinsonian LRRK2 G2019S mutation carriers. Neurology 2011;77(4):325-33.

6. van der Vegt JP, van Nuenen BF, Bloem BR, Klein C, Siebner HR. Imaging the impact of genes on Parkinson's disease. Neuroscience 2009;164(1):191-204.

7. Adams JR, van Netten H, Schulzer M, et al. PET in LRRK2 mutations: comparison to sporadic Parkinson's disease and evidence for presymptomatic compensation. Brain 2005;128(Pt 12):2777-85.

8. Sierra M, Sanchez-Juan P, Martinez-Rodriguez MI, et al. Olfaction and imaging biomarkers in premotor LRRK2 G2019S-associated Parkinson disease. Neurology 2013;80(7):621-6.

9. Reetz K, Tadic V, Kasten M, et al. Structural imaging in the presymptomatic stage of genetically determined parkinsonism. Neurobiol Dis 2010;39(3):402-8.

10. Brockmann K, Groger A, Di Santo A, et al. Clinical and brain imaging characteristics in leucine-rich repeat kinase 2-associated PD and asymptomatic mutation carriers. Mov Disord 2011;26(13):2335-42.

11. Thaler A, Mirelman A, Helmich RC, et al. Neural correlates of executive functions in healthy G2019S LRRK2 mutation carriers. Cortex 2013;49(9):2501-11.
12. van Nuenen BF, Helmich RC, Ferraye M, et al. Cerebral pathological and compensatory mechanisms in the premotor phase of leucine-rich repeat kinase 2 parkinsonism. Brain 2012;135(Pt 12):3687-98.
13. Helmich RC, Thaler A, van Nuenen BF, et al. Reorganization of corticostriatal circuits in healthy G2019S LRRK2 carriers. Neurology 2015;84(4):399-406.
14. Gaig C, Ezquerra M, Marti MJ, Munoz E, Valldeoriola F, Tolosa E. LRRK2 mutations in Spanish patients with Parkinson disease: frequency, clinical features, and incomplete penetrance. Arch Neurol 2006;63(3):377-82.
15. Goetz CG, Tilley BC, Shaftman SR, et al. Movement Disorder Society-sponsored revision of the Unified Parkinson's Disease Rating Scale (MDS-UPDRS): scale presentation and clinimetric testing results. Mov Disord 2008;23(15):2129-70.
16. Doty RL, Bromley SM, Stern MB. Olfactory testing as an aid in the diagnosis of Parkinson's disease: development of optimal discrimination criteria. Neurodegeneration 1995;4(1):93-7.
17. Zigmond AS, Snaith RP. The hospital anxiety and depression scale. Acta Psychiatr Scand 1983;67(6):361-70.
18. Beck AT SRA, & Brown, G.K. TX: Psychological corporation. Manual for the Beck depression Inventory. 1996.
19. Visser M, Marinus J, Stiggelbout AM, Van Hilten JJ. Assessment of autonomic dysfunction in Parkinson's disease: the SCOPA-AUT. Mov Disord 2004;19(11):1306-12.

20. Folstein MF, Folstein SE, McHugh PR. "Mini-mental state". A practical method for grading the cognitive state of patients for the clinician. J Psychiatr Res 1975;12(3):189-98.

21. Fischl B, Salat DH, Busa E, et al. Whole brain segmentation: automated labeling of neuroanatomical structures in the human brain. Neuron 2002;33(3):341-55.

22. Douaud G, Smith S, Jenkinson M, et al. Anatomically related grey and white matter abnormalities in adolescent-onset schizophrenia. Brain 2007;130(Pt 9):2375-86.

23. Power JD, Barnes KA, Snyder AZ, Schlaggar BL, Petersen SE. Spurious but systematic correlations in functional connectivity MRI networks arise from subject motion. Neuroimage 2012;59(3):2142-54.

24. Liu Y, Liang M, Zhou Y, et al. Disrupted small-world networks in schizophrenia. Brain 2008;131(Pt 4):945-61.

25. Winkler AM, Ridgway GR, Webster MA, Smith SM, Nichols TE. Permutation inference for the general linear model. Neuroimage 2014;92:381-97.

26.Abdi, H. (2007). Bonferroni and sidak corrections for multiple comparisons. In N. J. Salkind (Ed.), Encyclopedia of measurement and statistics (pp. 103-107). Thousand Oaks (CA): Sage.

27. Sharman M, Valabregue R, Perlbarg V, et al. Parkinson's disease patients show reduced cortical-subcortical sensorimotor connectivity. Mov Disord 2013;28(4):447-54.

28. Hacker CD, Perlmutter JS, Criswell SR, Ances BM, Snyder AZ. Resting state functional connectivity of the striatum in Parkinson's disease. Brain 2012;135(Pt 12):3699-711.

29. Agosta F, Caso F, Stankovic I, et al. Cortico-striatal-thalamic network functional connectivity in hemiparkinsonism. Neurobiol Aging 2014;35(11):2592-602.

30. Luo C, Song W, Chen Q, et al. Reduced functional connectivity in early-stage drug-naive Parkinson's disease: a resting-state fMRI study. Neurobiol Aging 2014;35(2):431-41.

31. Ellmore TM, Castriotta RJ, Hendley KL, et al. Altered nigrostriatal and nigrocortical functional connectivity in rapid eye movement sleep behavior disorder. Sleep. 2013 Dec 1;36(12):1885-92.

32. Iranzo A, Fernández-Arcos A, Tolosa E, et al. Neurodegenerative disorder risk in idiopathic REM sleep behavior disorder: study in 174 patients. PLoS One. 2014 Feb 26;9(2):e89741.

33. Chai XJ, Castañón AN, Ongür D, Whitfield-Gabrieli S. Anticorrelations in resting state networks without global signal regression. Neuroimage. 2012 Jan 16;59(2):1420-8.

34. Fox MD, Snyder AZ, Vincent JL, Corbetta M, Van Essen DC, Raichle ME. The human brain is intrinsically organized into dynamic, anticorrelated functional networks. Proc Natl Acad Sci U S A. 2005 Jul 5;102(27):9673-8.

35. Baggio HC, Segura B, Sala-Llonch R, et al. Cognitive impairment and resting-state network connectivity in Parkinson's disease. Hum Brain Mapp. 2015 Jan;36(1):199-212.

36. Sheline YI, Raichle ME, Snyder AZ, et al. Amyloid plaques disrupt resting state default mode network connectivity in cognitively normal elderly. Biol Psychiatry 2010;67(6):584-7.

37. Harrington DL, Rubinov M, Durgerian S, et al. PREDICT-HD investigators of the Huntington Study Group, Rao SM. Network topology and functional connectivity

disturbances precede the onset of Huntington's disease. Brain. 2015 Aug;138(Pt 8):2332-46. 36.

38. Pereira JB, Ibarretxe-Bilbao N, Marti MJ, Compta Y, Junqué C, Bargallo N, Tolosa E. Assessment of cortical degeneration in patients with Parkinson's disease by voxel-based morphometry, cortical folding, and cortical thickness. Hum Brain Mapp. 2012 Nov;33(11):2521-34.

39. Thaler A, Artzi M, Mirelman A, et al. A voxel-based morphometry and diffusion tensor imaging analysis of asymptomatic Parkinson's disease-related G2019S LRRK2 mutation carriers. Mov Disord. 2014 May;29(6):823-7.

40. Parisiadou, Neurobiology of Disease, 29(44) p13971-13980, Parisiadou, Nature Neuroscience, vol 17, 2014, p367.

Table 1. Demographic and clinical data.

	Asymptomatic *LRRK2* mutation carriers (n=18)	**Asymptomatic noncarriers** (n=18)	Test stat/p
Age, years	43.33 ± 12.07	44.72 ± 12.48	0.339/0.736
Gender, % male	9 (50%)	7 (38.9%)	0.450χ/0.502
Mutation, n (%)			
G2019S	13 (72.2%)	NA	
R1441C	2 (11.1%)		
R1441G	3 (16.7%)		
Years of education	13.44 ± 5.08	15.28 ± 4.66	1.128/0.267
UPDRS I score	2.89 ± 4.52	2.39 ± 3.70	157.5§/0.881
UPDRS II score	0.22 ± 0.43	0.28 ±0.58	160.0§/0.930
UPDRS III score	0.39 ± 0.98	0.06 ±0.24	134.5§/0.147
UPSIT score	32.72 ± 3.74	33.0 ± 3.45	0.232/0.818
SCOPA-AUT score	8.44 ± 6.68	7.56 ± 4.88	0.456/0.651
HADS total score	8.0 ± 5.69	7.83 ± 6.05	0.085/0.933
HADS Anxiety score	5.17 ± 3.26	5.39 ± 3.24	0.205/0.839
HADS Depression score	2.83 ± 2.68	2.44 ± 3.37	0.383/0.704
BDI	5.12 ± 6.19	4.06 ± 4.87	0.566/0.575
MMSE score	29.17 ± 0.92	29.17 ± 0.99	159.5§/0.932

Results are described by mean ± SD. Test statistics (Test stat) refer to Student's t, Mann-Whitney's U (§) or Pearson's chi-square (χ).

BDI: Beck Depression Inventory-II. HADS: Hospital Anxiety and Depression Scale. MMSE: Mini-mental state examination. SCOPA-AUT: Scales for Outcomes in Parkinson's disease – Autonomic. UPDRS: unified Parkinson's disease rating scale. UPSIT: University of Pennsylvania Smell Identification Test. NA: not applicable

Table 2. Differential connectivity in asymptomatic *LRRK2* mutation carriers and noncarriers.

Topography (maximum)	Volume (mm^3)	Voxels	MNI coordinates	p-value
Right substantia nigra seed				
Right occipital pole	9344	146	14, -94, 20	0.003
Right occipital pole	768	12	26, -94, -12	0.008
Right lateral occipital cortex	640	10	46, -62, 8	0.037
Right lateral occipital cortex	576	9	50, -78, -16	0.038
Left striatum, caudal motor region seed				
Superior parietal lobule	2368	37	-30, -70, 52	0.019
Precuneus	1728	27	-6, -58, 60	0.013

Description of clusters of significant between-group functional connectivity differences ($p<0.05$ FWE-corrected). Asymptomatic *LRRK2* mutation carriers showed reduced left striatocortical and increased right nigrocortical connectivity compared with noncarriers. MNI coordinates: x, y, z MNI coordinates of the maximum.

Table 3. Correlations between subcortical volumes and both age and connectivity measures.

	Left caudal motor striatal connectivity (rho/p)		**Age (rho/p)**	
	***LRRK2* mutation carriers**	***LRRK2* mutation noncarriers**	***LRRK2* mutation carriers**	***LRRK2* mutation noncarriers**
Mean striatal volume	0.63/0.007	0.05/0.842	-0.67/0.003	-0.23/0.382
L caudate	0.65/0.004	0.07/0.801	-0.54/0.024	-0.14/0.592
L putamen	0.53/0.029	0.05/0.861	-0.65/0.005	-0.21/0.425
R caudate	0.61/0.010	-0.01/0.997	-0.52/0.031	-0.2/0.442
R putamen	0.57/0.018	0.07/0.805	-0.68/0.003	-0.24/0.354

Left caudal motor striatal connectivity: mean Z scores in the clusters of significant intergroup differences in connectivity with the caudal motor subdivision of the left striatum. *Mean striatal volume*: average of bilateral caudate and putaminal volumes. *L*: left. *R*: right. *rho*: partial correlation coefficient (controlling for intracranial volume).

Figure legends

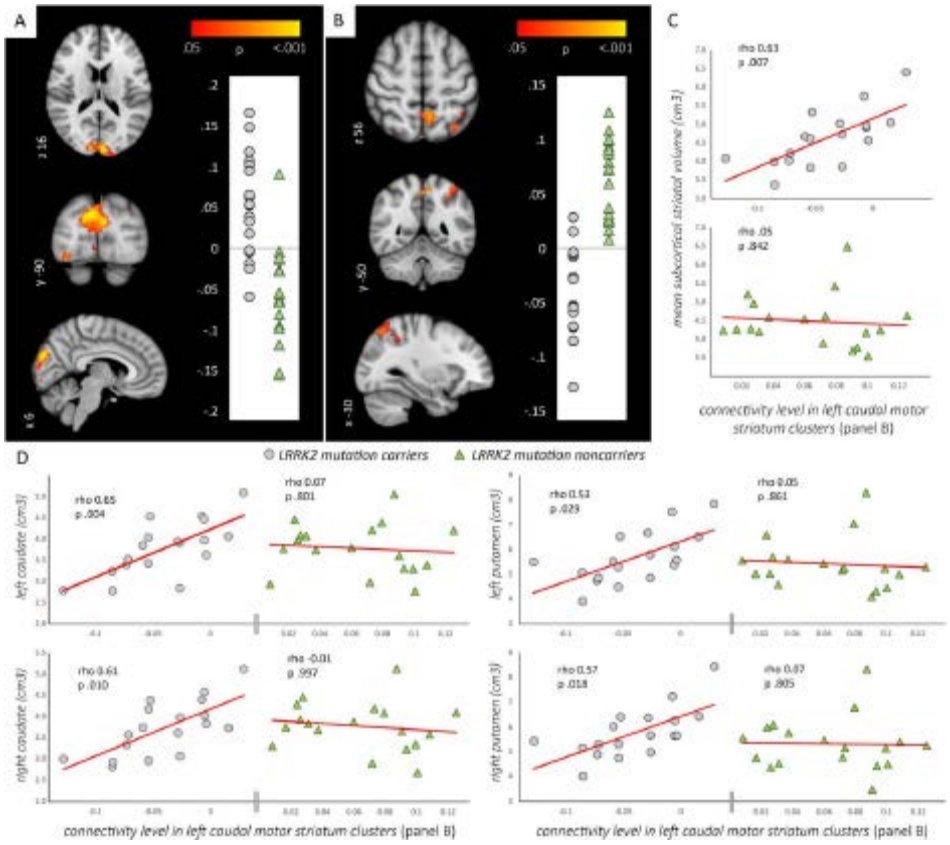

Fig 1. Differential resting-state functional connectivity between asymptomatic *LRRK2* mutation carriers and noncarriers and correlations with striatal volumes. **Panels A and B:** Color clusters indicate areas of significant increases in connectivity of the right substantia nigra (panel A) and connectivity reductions of the caudal motor subdivision of the left striatum (panel B) in mutation carriers ($p<0.05$, FWE correction). Plots show the distribution of mean connectivity values in the regions where significant intergroup differences were found, according to group. The Montreal Neurological Institute coordinates of the slices shown are indicated. **Panels C and D:** Plots show the relationship between connectivity levels (in the clusters shown in panel B) and striatal volumes (panel C: mean striatal volume; panel D: right and left caudate nuclei and putamina). Significant correlations were observed in the *LRRK2* mutation group only. R: right. L: left. P: posterior. In plots, *LRRK2* mutation

carriers are represented by gray circles; mutation noncarriers are indicated by green triangles.

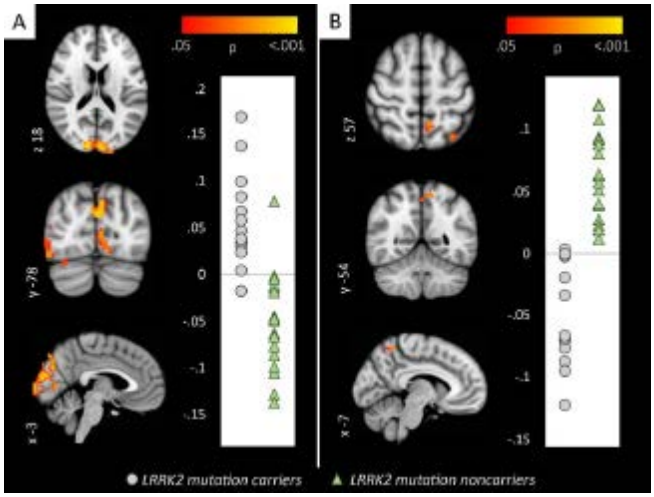

Fig 2. Differential resting-state functional connectivity between asymptomatic G2019S LRRK2 mutation carriers and noncarriers.

Color clusters indicate areas of significant increments in connectivity of the right substantia nigra (panel A) and connectivity reductions of the caudal motor subdivision of the left striatum (panel B) in mutation carriers ($p<0.05$, FWE correction). Plots show the distribution of mean connectivity values in the regions where significant intergroup differences were found, according to group. *LRRK2* mutation carriers are represented by gray circles; mutation noncarriers are indicated by green triangles. The Montreal Neurological Institute coordinates of the slices shown are indicated. R: right. L: left. P: posterior.